

Supporting Information

Electrokinetic assembly of one-dimensional nanoparticle chains with cucurbit[7]uril controlled sub-nanometer junctions

*Nina Hüskén,[†] Richard W. Taylor,[‡] Dodzi Zigah,[†] Jean-Christophe Taveau,[§] Olivier Lambert,[§]
Oren A. Scherman,⁺ Jeremy J. Baumberg,[‡] Alexander Kuhn^{*†}*

* kuhn@enscbp.fr

[†] Université de Bordeaux 1, Institut des Sciences Moléculaires UMR 5255, Groupe Nanosystèmes Analytiques, Site ENSCBP, 16 avenue Pey Berland, 33607 Pessac, France.

[‡] NanoPhotonics Centre, Cavendish Laboratory, University of Cambridge, Cambridge CB3 0HE, U.K.

[§] Institut de Chimie et Biologie des Membranes et des Nanoobjets, Université de Bordeaux, CNRS, UMR 5248, 33600 Pessac, France.

⁺ Melville Laboratory for Polymer Synthesis, Department of Chemistry, University of Cambridge, Cambridge, CB2 1EW, U.K.

I. Membrane Cells

a) Membrane Cell for TEM Analysis

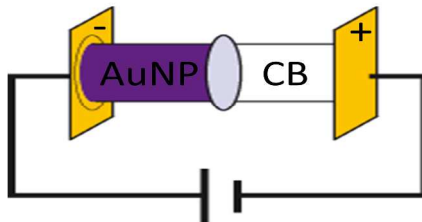


Figure S1. Setup for used TEM measurements.

Figure S1 shows the set-up of the membrane cell. The cell consists of two chambers, which are prepared from 1 mL polypropylene syringes, to yield two cylindrical compartments with a length of 1 cm each. These compartments are glued each with a silicon glue to a planar gold electrode, which is soldered with a copper wire to enable electrical connection. The SPITM-Pore standard white polycarbonate (PC) membranes are purchased from SPI[®] supplies and have nanopores with an average diameter of 30 nm, a nanopore density of 6×10^8 pores/cm² and a nominal thickness of 6 μ m. A square of 1×1 cm² of the membrane is glued between the two compartments with silicone glue to yield the sandwich type cell shown in Figure S1. In order to facilitate introduction of the respective solutions into the two chambers, a small slot is cut into each chamber from above with an additional hole for air equilibrium.

b) Membrane Cell for real-time extinction spectroscopy

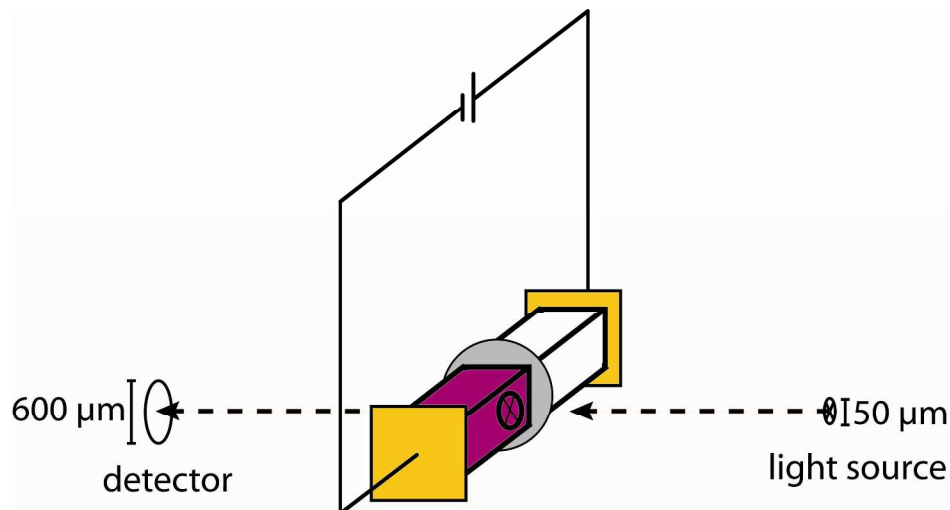


Figure S2. Setup for real-time extinction spectroscopy.

For the real-time extinction spectroscopy experiments a membrane cell was used, which was constructed analogously to the one used for the preparation of the TEM grids, except that the syringe-based reaction compartments were replaced by compartments produced from single use UV cuvettes. The beam of a white light source with a diameter of 50 μm was focused at the AuNP compartment as close to the membrane as possible, as shown in Figure S2.

II. Synthesis and Characterization of gold nanoparticles

a) AuNP Synthesis

The gold nanoparticles were synthesized according to the standard Turkevitch method, which yields citrate-stabilized AuNPs after reduction of HAuCl_4 with citrate.¹

b) Determination of AuNP Diameter

The diameter d of the AuNP was determined from TEM images by determining the Feret's diameter of 100 AuNP. Feret's diameter is defined as the distance between two parallel tangents of the

particle at an arbitrary angle to the horizontal axis of the TEM image. Here a fixed angle of 90° is used throughout in order to average over all arbitrary orientations of the particles with respect to the horizontal axis of the TEM image. AuNPs with particle sizes between 16 – 20 nm were used in this work, with a general deviation about ± 1.2 nm within one batch of AuNP.

c) Determination of AuNP concentration

The concentration of the synthesized AuNP, $c(\text{AuNP})$, was determined by UV/Vis spectroscopy. Therefore a UV/Vis spectrum was recorded between $\lambda = 190 - 900$ nm against a background of milli-Q water and the absorbance A^m at the absorbance maximum at $\lambda = 520$ nm of the surface plasmon resonance of the AuNP was recorded. The AuNP concentration was calculated based on the Beer-Lambert law $A^m = \varepsilon \cdot l \cdot c(\text{AuNP})$. The molar extinction coefficient ε depends on the AuNP diameter, and theoretical values for ε , which are calculated based on Mie theory,² are reported in the literature.³

III. AuNP/CB[7] reaction

a) Extinction spectroscopy of various CB[7]/AuNP ratios

The reaction between AuNPs and CB[7] was studied by mixing AuNPs and CB[7] in ratios indicated in Figure S3 (ratios between AuNP : CB[7] = 1:300 to 1:100000) at $t = 0$. UV spectra were recorded every 2 min over a time range of 60 min. Figure S3 shows the spectra at $t = 20$ min after mixing the respective AuNP/CB[7] ratio.

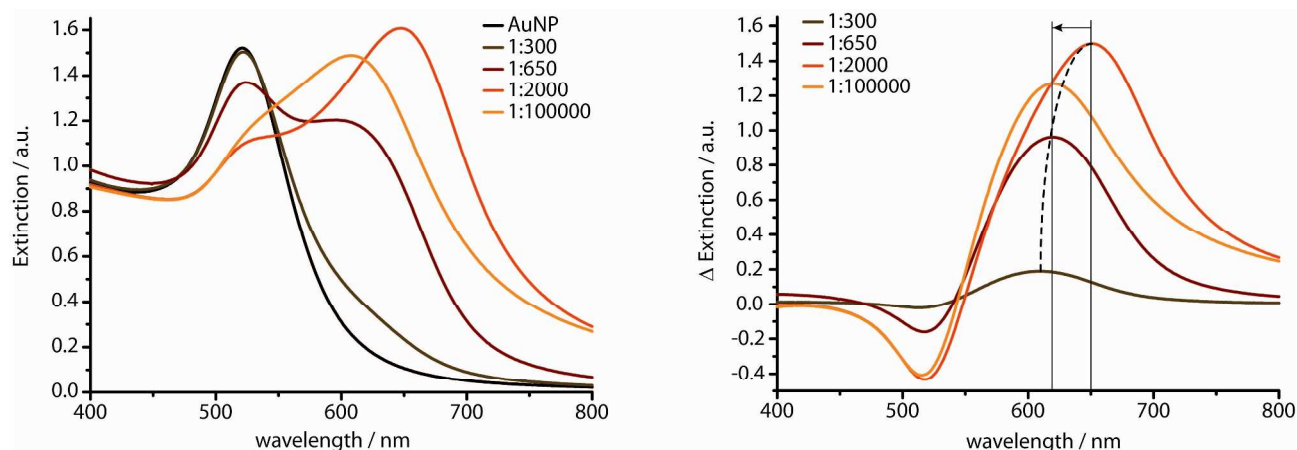


Figure S3. Extinction spectroscopy of suspensions of different CB[7]/AuNP ratios after $t = 20$ min (left: original data, right: difference spectra)

b) Extinction spectroscopy at different points in time

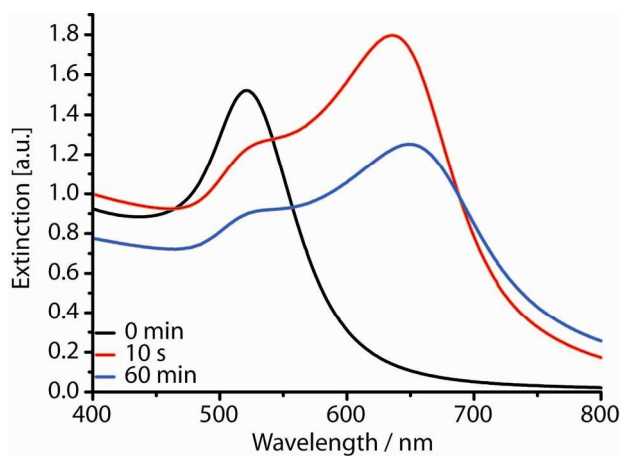


Figure S4. Extinction spectra of AuNP:CB[7] = 1:2000 at different points in time.

AuNPs and CB[7] are mixed in a ratio of 1 to 2000 and an extinction spectrum is measured every 2 mins. Figure S4 shows that the longitudinal mode is developed to its maximum already after $t = 10$ s and then continuously diminishes, which can be ascribed to the sedimentation of the formed

aggregates. This indicates, that the AuNP/CB[7] reaction is already finished within the first 10 s after mixing.

IV. TEM measurements

a) Standard TEM

All standard TEM measurements are performed at the Bordeaux Imaging Center BIC, (Université Bordeaux II, Bordeaux, France) on the instrument FEI TECNAI 12. For all measurements copper TEM grids with a Formvar/Carbon membrane are used, which were purchased from Agar Scientific (Essex, U.K.). The TEM grids were prepared by dipping the grid into the respective solution after the experiment in order to adsorb the formed aggregates onto the grid membrane.

b) Statistical Analysis

We analyzed at least 3 TEM grids per individual experiment and every TEM image we show in the manuscript was chosen to be representative for the chain or chain-type object with respect to its length and linearity for a given set of parameters. The discussed tendencies were reproduced twice in independent sets of experiments, using freshly synthesized nanoparticles whereas the CB solutions were throughout all experiments prepared from one stock solution. Experiments with the parameter set $T = \text{r.t.}$, $t = 30 \text{ min}$, $R = 4500$ have been even carried out significantly more often than for the other parameter sets, since it was used as a standard concerning reliability and reproducibility. We observed in this case that the deviations between 3 TEM grids prepared with chains obtained from the same experiment were comparable to those derived from different experiments carried out under identical conditions. This indicates that the preparation of the TEM grids has the biggest influence on the reproducibility, while the chain formation as such appears to have less impact. This is confirmed by the cryo-TEM and UV measurements, which show a good reproducibility of the chain formation. The statistical analysis presented in the main manuscript is

based on the analysis of at least 12 AuNP/CB[7] chains per experiment, which had a linearity factor f of at least 0.5 if it was not a clear structure of interconnected linear chains. The linearity factor f is defined as $f = \text{NP}_{\text{chain}}/\text{NP}_{\text{agg}}$ (NP_{chain} = AuNPs bound in a linear chain; NP_{agg} = total number of AuNP bound in a chain-type aggregate). The linearity factor calculated for the series of different voltages, as discussed for Figure 4A in the main manuscript is demonstrated in Figure S5.

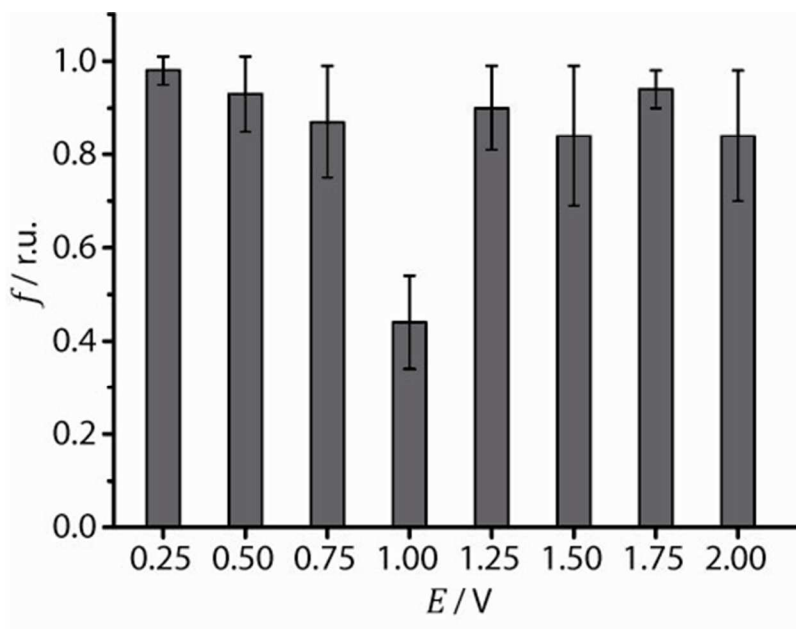


Figure S5. Linearity factors calculated for different applied DC potentials between $E = 0.25 - 2 \text{ V}$.

An increase in the reaction time at a constant voltage of $E = 0.85 \text{ V}$ in contrast does not reveal a clear tendency and the linearity factor remains largely constant with an average value of $f = 0.75 \pm 0.09$.

b) Cryo-TEM

The Cryo-TEM measurements are performed with a high-resolution cryo transmission electron microscope FEI TECNAI F20 (FEG) equipped with a Gatan 2k x 2k USC 1000 slow-scan CCD

camera for low light level. For the calculation of the 3D models shown in the main manuscript, images are recorded at three different angles ($\alpha = -15^\circ, 0^\circ, +15^\circ$). Each of the image triplets are noise-reduced and thresholded before extracting the 2D gravity centers of the nanoparticles using ImageJ⁴. Then, from all the combinations of pairs of TEM images, the 3D centers of gravity are calculated and averaged according to classical stereoscopic formulas based on trigonometry as previously described⁵. For the rendering, the 3D models of the chains are then converted into voxels spheres and displayed as isosurfaces with chimera⁶. The inter-particle distances are automatically measured from the denoised and thresholded 0° -tilted TEM images. This width corresponds to a line segment delineated between two adjacent particles and passing through their 2D gravity centers. All the image processing and analysis is performed with lab-made JavaScript scripts for ImageJ.

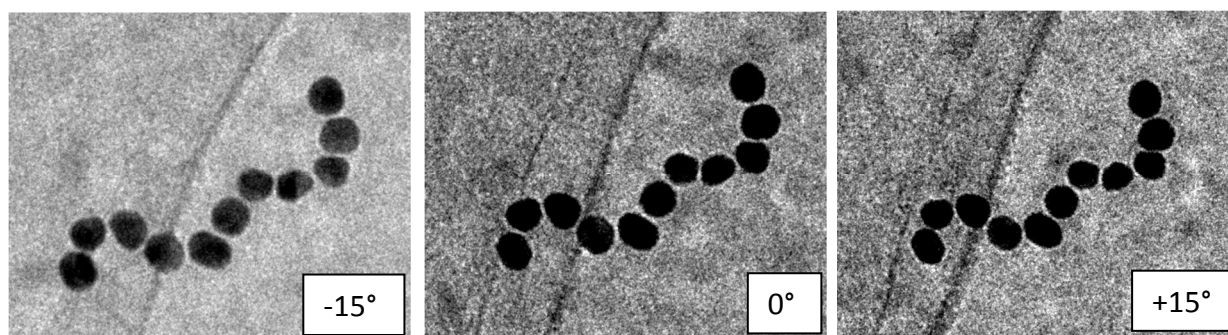


Figure S6. Cryo-TEM images of a chain at three different tilt angles α , which were the basis for the calculation of the 3D image shown in Figure 9A of the main manuscript.

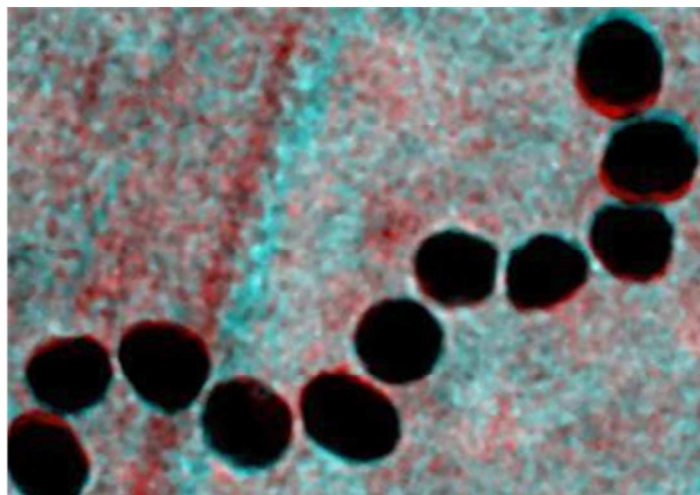


Figure S7. Red/green 3D cryo-TEM image, which corresponds to the cryo-TEM images shown in Figure 9A of the main manuscript

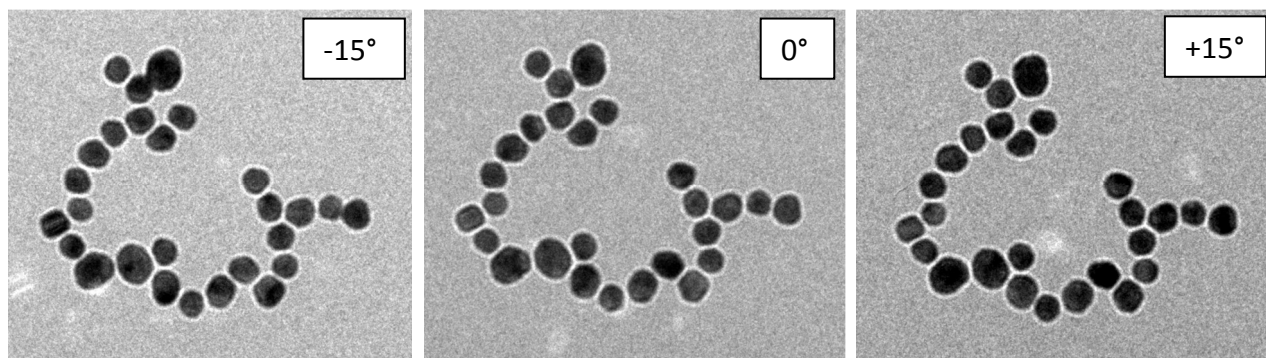


Figure S8. Cryo-TEM images of a branched chain at three different tilt angles α , which were the basis for the calculation of the 3D image shown in Figure 9B of the main manuscript.

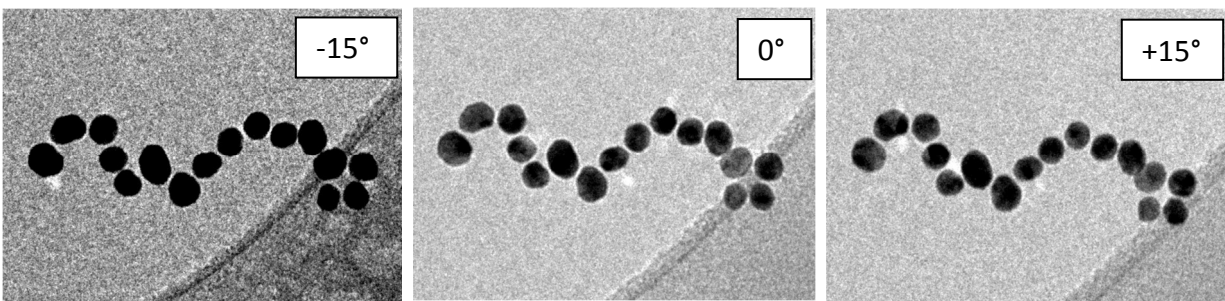


Figure S9. Cryo-TEM images of a linear 16AuNP chain at three different tilt angles α , which were the basis for the calculation of the 3D image shown in Figure S10.

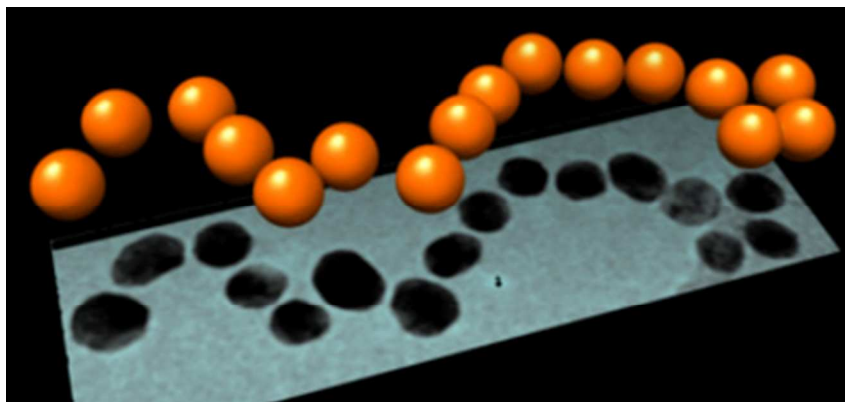


Figure S10. 3D-image of an AuNP/CB[7] chain (orange spheres) with a length of 16 AuNP calculated from Cryo-TEM images, which were recorded at three different tilt angles $\alpha = -15, 0, +15$ and are shown in the background.

c) TEM image of a long chain

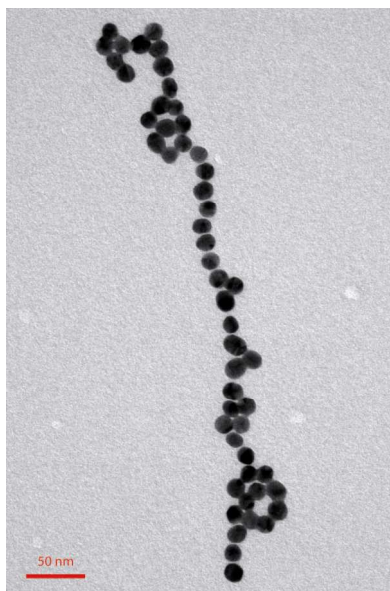


Figure S11. AuNP/CB[7] chain of about 50 nm.

V. Extinction spectroscopy

Extinction spectroscopy was performed in the Nanophotonics Centre of the Cavendish Laboratory at the University of Cambridge, UK. The cell was incorporated in an optical system between two lenses. Light source ($\varnothing = 50 \mu\text{m}$) and detector ($\varnothing = 600 \mu\text{m}$) were placed on opposing sides of the focal point of the respective lens (see Figure S12) in order to collimate the light through the cell and finally focus onto the detector. The data were processed and analyzed with the software IGOR (Wavemetrics).

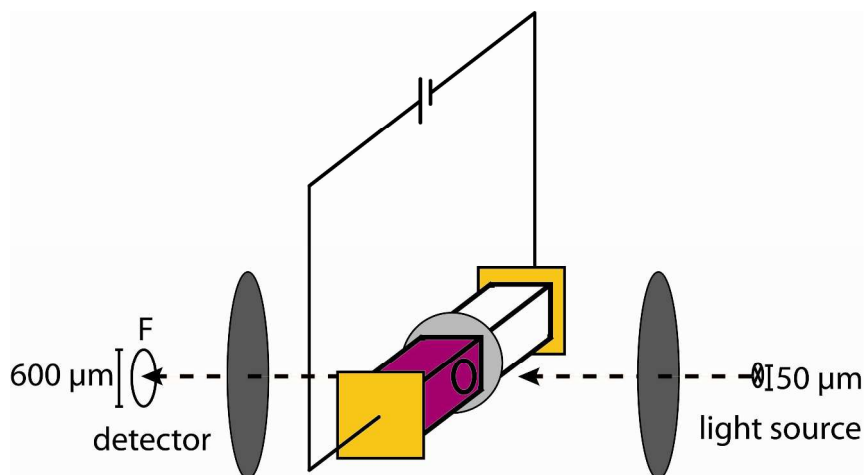


Figure S12. Set-up for real-time extinction measurements.

References

- [1] Turkevich, J.; Stevenson, P. C.; Hillier, J. *Discuss. Faraday. Soc.* 1951, 11, 55-75.
- [2] Mie, G. *Ann. Phys.* 1908, 25, 377-445.
- [3] Haiss, W.; Thanh, N. T. K.; Aveyard, J.; Fernig, D. G. *Anal. Chem.* 2007, 79, 4215-4221.
- [4] Rasband, W.S.; ImageJ, U. S. National Institutes of Health, Bethesda, Maryland, USA, <http://imagej.nih.gov/ij/>, 1997-2012.
- [5] Hein L.R. *J. Microsc.* 2001, 204, 17-28.
- [6] Pettersen E.F.; Goddard T.D.; Huang C.C.; Couch G.S.; Greenblatt D.M.; Meng E.C.; Ferrin T.E. *J. Comput. Chem.* 2004, 25, 1605-12.